A comparative study of simulated body fluids in the presence of proteins

Weitian Zhao, Jacques Lemaître and Paul Bowen

Powder Technology Laboratory, Institute of Materials, École Polytechnique Fédérale de Lausanne (EPFL), 1015 Lausanne, Switzerland

Abstract

Simulated body fluid (SBF) is widely used as part of an *in vitro* method to evaluate implant materials such as their apatite forming ability (AFA), a typical indication of potential bone-bonding ability *in vivo*. We report the use of carbonate-buffered SBFs as potential solutions for implant evaluation and the effect of proteins, represented by bovine serum albumin (BSA) in SBFs on the nucleation and growth of hydroxyapatite (HA). These solutions are buffered by the thermodynamic equilibrium with 5% CO_2 in an incubator, and result in a deposition of carbonated HA. Using several titanium-based surfaces, these solutions were studied in comparison with the widely-used SBF (ISO 23317). The presence of BSA strongly inhibited the formation of HA in traditional SBF, while HA can still be observed in carbonate-buffered SBFs. A kinetic study reveals that the inhibitory effect is concentration dependent with 0.1g/L and 1g/L of BSA having little effect on HA growth but a complete inhibition of HA formation at 5g/L of BSA, as tested using NaOH treated titanium with a known positive AFA. The decrease in solution pH and free calcium concentrations in SBFs due to the addition of BSA is not significant, suggesting other causes for the strong inhibitory effect.

Keywords
Bioactivity, Hydroxyapatite, SBF, Protein, Titanium

1. Introduction

The discovery of bone-bonding glass in the 70s by Hench *et al.* opened up new possibilities in bioactive implant materials, attracting many research activities and leading to the developments of various commercial products [1][2] Instead of being passively implanted and often encapsulated by fibrous tissues, these materials can actively form a direct bonding with the surrounding bone, thus significantly increasing the implant fixation and the long-term stability. The rapid development of new potential implant materials presents both scientific and technical challenges for the design of a fast assessment method other than traditional animal experiments for implant evaluation.

Kokubo *et al.* proposed an *in vitro* method using an acellular solution with inorganic ion composition and pH similar to biological fluids called simulated body fluid (SBF) to test new implants [3][4]. The method is based on the observations that a bonelike apatite layer is often found between bioactive implants and the surrounding bone, acting as a key component for osseointegration [5]. Thus the question of material bioactivity (which hereafter refers to the bone-bonding ability), reduces to the apatite forming ability (AFA) of a material *in vivo*. It is further assumed that the apatite forming behavior *in vivo* can be reproduced using an artificial solution supersaturated with respect to hydroxyapatite (HA) *in vitro*, meaning that a material exhibiting HA deposition in SBF would indicate its bone-bonding ability. In 2007, the testing protocol of this *in vitro* method was standardized by the International Organization for Standardization (ISO 23317) and since then has been widely used as a method to evaluate various implant materials [4][6][7][8]. Despite its success, the simplifications of using a solution to mimic the body fluid and determining the bioactivity by the AFA also result in several limitations, which should be pointed out.

1. The bone bonding/formation process is essentially determined by osteoblasts, the activity of which is regulated by various local factors including both inorganic ions as well as organic growth factors. Although the formation of a bone-like apatite layer likely facilitates the proliferation and activity of osteoblasts, which could eventually lead to the formation of bone, other possible mechanisms of bioactivity also exist. These include bioactivity from specific interactions with osteoblasts/stem cells of biofunctional materials by either releasing certain biomolecules or possessing special surface topographical features [9][10]. The existence of other possible mechanisms might explain some cases of inconsistency between *in vitro* predictions and *in vivo* results [11].

2. Assuming the bone-bonding is achieved by the formation of an apatite layer, a qualitative correlation between a material's apatite forming ability *in vivo* and its bone-bonding strength is still difficult to establish. That is, a higher AFA *in vivo* does not necessarily lead to a stronger bonding. This is due to many other factors determining the final bonding strength including surface mechanical properties (adhesion between surface porous layer and bulk implant), and surface roughness, which is typically observed to be a critical factor in animal experiments [12][13].

If we limit the discussion to the chemical route (through the formation of HA) to bioactivity and focus on the *in vitro* method to predict *in vivo* AFA, there are still some issues that remain to be understood. The major criticism of the method is the lack of organics, especially proteins, which are abundant in human blood plasma (roughly 70 g/L in human blood plasma [14]) and are well-known to have specific/non-

specific adsorption on various surfaces, which could affect the nucleation & growth of apatite in SBF [15][16][17][18][19][20]. In fact, proteins, along with other organic molecules, are also active players in the regulation of the biomineralization processes *in vivo* [21]. Despite the existence of a number of *in vitro* studies on the effect of proteins, their role as promotors or inhibitors for calcium phosphate nucleation and growth is still unclear. The reported discrepancies come from varying experimental methodologies used in the literature, as well as other factors including protein concentration and conformation [22][23]. In terms of the heterogeneous nucleation/growth of HA on Ti-based implants in SBF, only a few papers can be found but no clear conclusions can be made due to the use of different SBF compositions and operating procedures [24][25].

Also, the current SBF (ISO 23317) uses tris(hydroxymethyl)aminomethane (($CH_2OH)_3CNH_2$, Tris) to buffer the solution pH, while Tris is not a component of human blood plasma and might have an effect on calcium phosphate nucleation [26]. The human blood is buffered by the equilibrium between carbonates and 5% partial pressure of CO_2 in blood serum [27]. Due to the high structural variability of apatite crystals, the presence of carbonate species in solution will result in carbonate incorporation into the apatite lattice by either substituting the hydroxyl groups (type A) or occupying the phosphate position (type B) [28][29][30], as it is the case for apatite in natural bone [31]. Furthermore, it has also been demonstrated that carbonate complexes could lead to an increased apparent solubility of HA [32]. Despite being proposed in a review by Bohner and Lemaitre [15], unfortunately, so far there has been very limited studies using carbonate-buffered SBFs solutions for implant evaluation.

This paper aims to fill this gap and address the above-mentioned issues, namely the performance of a carbonate-buffered SBF versus the SBF proposed by Kokubo [8] and the effect of proteins on the nucleation and growth of apatite from SBF. Two new solution compositions are proposed and their ability to nucleate apatite on different representative titanium-based surfaces are compared with Kokubo's SBF, with or without the addition of protein, represented by bovine serum albumin (BSA). The effect of proteins on the kinetics of HA formation is also investigated at different protein concentrations. The changes in solution pH and free calcium ion concentrations in the presence of proteins are measured to help interpret the results. These studies aim to address the remaining questions in the field, the answers of which could lead to a better understanding of the system and help better interpret the results produced using SBFs.

2. Materials and Methods

2.1 Sample preparation

Four different titanium-based surfaces were chosen for this study: i) sandpaper-polished titanium, ii) titanium - polished and heat-treated in air, iii) titanium - polished and treated with NaOH solution, and iv) titanium - polished, NaOH treated and heated in air. Commercial pure (CP) grade 1 titanium discs (Hempel Special Metals, Switzerland) of 19 mm $\times$ 1.5 mm were all machine polished before any chemical treatment. The polishing was applied on both sides of the discs using silicon carbide P320, P1200, and 1200/4000 abrasive paper consecutively, followed by washing with acetone, water and ethanol in an ultrasonic bath. The NaOH treatment was conducted using 5M NaOH solution for 24h at 60°C. Afterwards, the discs were washed using flowing de-ionized water for about 30s and then dried. The heat treatment was applied at 600°C (heating rate 100°C/h, natural cooling) for an hour in ambient atmosphere.

2.2 Design and preparation of simulated body fluids

A thermodynamic model was used to design SBFs with a target pH of 7.40 at testing conditions. More details about this model are given in the supporting information (SI–1). Two new SBFs are proposed and the compositions in comparison with human blood plasma ionic concentration are given in Table 1. SBF-BCS1 was prepared by mixing equal volumes of two stock solutions A (containing NaCl, NaHCO$_3$, Na$_2$HPO$_4$·2H$_2$O and Na$_2$SO$_4$) and B (containing NaCl, MgCl$_2$·6H$_2$O, CaCl$_2$ and HCl). SBF-BCS2 was prepared in a similar manner with additional KCl in solution B and a slightly different ionic concentration. The detailed recipe is given in the supporting information (SI–2). The purpose of using two stock solutions is to separate calcium and phosphate ions before the AFA test to avoid undesired nucleation in a solution supersaturated with respect to several calcium phosphate phases. Both SBF-BCS1 and SBF-BCS2 (hereafter abbreviated as BCS-1 and BCS-2) were designed to be used under 5% CO$_2$ at 36.5°C. Kokubo's corrected SBF (c-SBF) was prepared by strictly following the procedures of ISO 23317:2014 [8]. The solution was prepared using NaCl, NaHCO$_3$, KCl, K$_2$HPO$_4$·3H$_2$O, MgCl$_2$·6H$_2$O, CaCl$_2$, and Na$_2$SO$_4$ and buffered by Tris and HCl solution at 36.5°C. The final ionic concentrations are given in Table 1.

Table 1. Compositions of SBFs and human blood plasma.

Ion	Human Blood Plasma [27] Total	Dissociated	c-SBF	BCS-1	BCS-2
Na^+	142.0	142.0	142.0	143.00	142.0
K^+	5.0	5.0	5.0	--	5.0
Mg^{2+}	1.5	1.0	1.5	1.50	1.5
Ca^{2+}	2.5	1.3	2.5	2.31	2.5
Cl^-	103.0	103.0	147.8 [a]	124.64 [a]	129.4 [a]
HCO_3^-	27.0	27.0	4.2	22.20	22.6
HPO_4^{2-}	1.0	1.0	1.0	1.39	1.0
SO_4^{2-}	0.5	0.5	0.5	0.50	0.5
Additional					
TRIS	--	--	0.05	--	--
HCl	--	--	40.0	0.96	1.2

Header note: Concentration [mM]

[a] The chloride ion concentration does not include added HCl solution as pH buffer.

In the study of proteins in SBF, bovine serum albumin (lyophilized powder, ≥ 96%, Sigma-Aldrich) was added to c-SBF, BCS-1 and BCS-2 (both in solution B) with 0.2 g antibacterial agent NaN_3 per 1L SBF. The pH values of solution BCS-1 and BCS-2 were measured using a pH meter (FiveEasy Plus, Mettler Toledo) under 5% CO_2 at 36.5°C four times at each BSA concentration.

2.3 Apatite forming ability (AFA) test

The AFA test was conducted by suspending the sample discs with an inert stainless steel wire and immersing in 50 mL SBF in a test tube. The volume of SBF used is based on a recommended solution volume/material surface ratio ($v_s = 100 \cdot S$, [mm]) proposed in ISO 23317 [8]. BCS-1 and BCS-2 were prepared by manually mixing the solutions A and B using a twin syringe connected with a static mixer, while c-SBF was used as prepared. All solutions were used within one day of preparation. Detailed procedures for solution preparation and AFA test procedures can be found in the operating protocols attached in the supporting information SI–2. It should be noted in particular that due to a high carbonate concentration and a higher CO_2 partial pressure in solution A compared to the atmosphere, it is recommended to use fresh as-prepared solutions to avoid carbonate loss during storage and handling, which could lead to an increase in solution pH and eventually possible undesired apatite formation when mixed with solution B, irrespective of the presence of any testing materials. After the immersion of the samples, in the case of BCS-1 and BCS-2, the tubes were transferred into an incubator with 5% CO_2 partial pressure and a constant temperature of 36.5°C for the testing time before removal. Samples tested in c-SBF were put

in an oven at 36.5℃. After the test, the discs were gently washed with water and ethanol and dried for surface characterization.

2.4 Surface characterization

X-ray diffraction (XRD) analysis was conducted using a Philips X'Pert X-ray diffractometer with Cu K radiation (Kα1, λ = 1.5406 Å) operating at 45 kV and 40 mA. Crystal structures of the tested materials were identified using standard profiles from the JCPDS database. Surface morphologies were observed by scanning electron microscopy (SEM, Merlin (GEMINI II), Zeiss). Samples were also analyzed by Fourier transform infrared spectroscopy (FTIR, Nicolet 6700, Thermo Fisher Scientific) in attenuated total reflection (ATR) mode.

2.5 Quantification of apatite deposition

The amount of apatite deposited was quantified by analyzing the calcium concentrations of the remaining SBFs after the AFA test. The sample discs were taken out and 1 vol% of 65 wt% concentrated HNO_3 was added to the solution to prevent possible further calcium phosphate precipitation. The elemental concentrations of the solutions were analyzed by inductively coupled plasma (ICP-OES, ICPE-9800, Shimadzu). In each group of measurements, as-prepared SBF was also introduced as a control and the amount of calcium or phosphate precipitated is then calculated as the difference with the value obtained from the control group.

2.6 Measurement of free calcium concentration in the presence of BSA

The free calcium concentrations of different solutions were measured using a calcium-selective electrode (perfectION Ca Combination Electrode, Mettler Toledo), calibrated with calcium standards at 10 mg/L, 100 mg/L and 1000 mg/L. Calcium solutions of 20 mL were measured without BSA and with BSA of different concentrations at 1g/L, 5g/L, 10g/L and 20g/L. The 20 mL solutions were prepared to have 100 mg/L of calcium by $CaCl_2$ and were buffered with 1 mmol Tris and 0.86 mL 1M HCl at physiological pH. An additional 2 vol% ionic strength adjuster (ISA) was added to both calibration solutions and testing solutions according to the device operating protocol. Each data point was measured two times. The solution pH was measured three times.

2.7 Statistical analysis

Statistically significant differences were identified using a multifactorial statistical model [33]. A type I error risk of 5% was used.

3. Results

3.1 Comparison of SBFs

BCS-1 is based on a proposed solution JL2 by Bohner and Lemaitre in 2009 with calcium and phosphate concentrations slightly different from c-SBF [15]. BCS-2 is tuned to have the same calcium and phosphate concentration as c-SBF, thus the main difference is the higher concentration of carbonates in equilibrium with 5% CO_2 serving as a pH buffer. The two proposed SBFs are designed with a calculated pH of 7.40 at the testing condition. The pH measurements at these conditions give a pH of 7.42 $\pm$ 0.02 for BCS-1, and 7.41$\pm$0.01 for BCS-2. The consistency with the calculated values validates the thermodynamic model used in this study (SI–1). A summary of BCS-1, BCS-2 and c-SBF is given in Table 2. The supersaturation S is defined as the ratio of the activity product of ion units composing the crystal to the corresponding solubility product K_{sp}.

Table 2. A comparison of different SBFs used. The common logarithms of supersaturation values of different minerals are calculated. Hydroxyapatite (HA): $Ca_5(PO_4)_3(OH)$; Octacalcium phosphate (OCP): $Ca_8H_2(PO_4)_6 \cdot 5H_2O$; Calcite: $CaCO_3$.

	BCS-1	BCS-2	c-SBF
$p(CO_2)$ [atm.]	5.0%	5.0%	1.0%
pH (calculated)	7.40	7.40	7.34 [a]
$\log(S_{HA})$	10.89	10.63	10.27
$\log(S_{OCP})$	6.31	5.69	3.64
$\log(S_{calcite})$	0.60	0.64	- 0.16

[a] The calculation is based on the assumption of a closed system, where exchange of CO_2 with the atmosphere is not allowed. During the actual preparation of c-SBF, CO_2 loss from the solution could take place. In equilibrium with the 0.04% CO_2 in air, the calculated pH is 7.51.

3.2 Apatite forming ability of four Ti surfaces in different SBFs

Four different titanium surfaces were chosen to study different SBFs with or without BSA. Chemical treatment using NaOH and heat treatment in air were investigated. According to the results reported in literature, an increasing order of AFA of the four surfaces is expected to be: as-polished titanium < heat treated titanium < NaOH and heat treated titanium < NaOH treated titanium [12][34][35]. The statistical design is presented in Table 3. The AFA test was conducted for 1 week.

Table 3. Statistical design of experiments

Factor	Definition	Levels		
		1	2	3
A	NaOH treatment	No	Yes	
B	Heat treatment	No	Yes	
C	SBF	BCS-1	BCS-2	c-SBF
D	BSA	No	Yes	
E	Replicate	1	2	

XRD patterns of the four surfaces before AFA test reveal different crystalline phases on the surface, as shown in Figure 1 and summarized in Table 4. Heat treatment induced TiO_2 rutile formation on the surface, while NaOH treatment led to the formation of a porous surface layer rich in Ti, Na and O, possibly forming a poorly crystalline $Na_{0.8}H_{1.2}Ti_3O_7$, which was further transformed by heat treatment into $Na_2Ti_6O_{13}$, TiO_2 rutile and possibly small amount of other sodium titanate phases. The results were similar to those reported in literature [36][37].
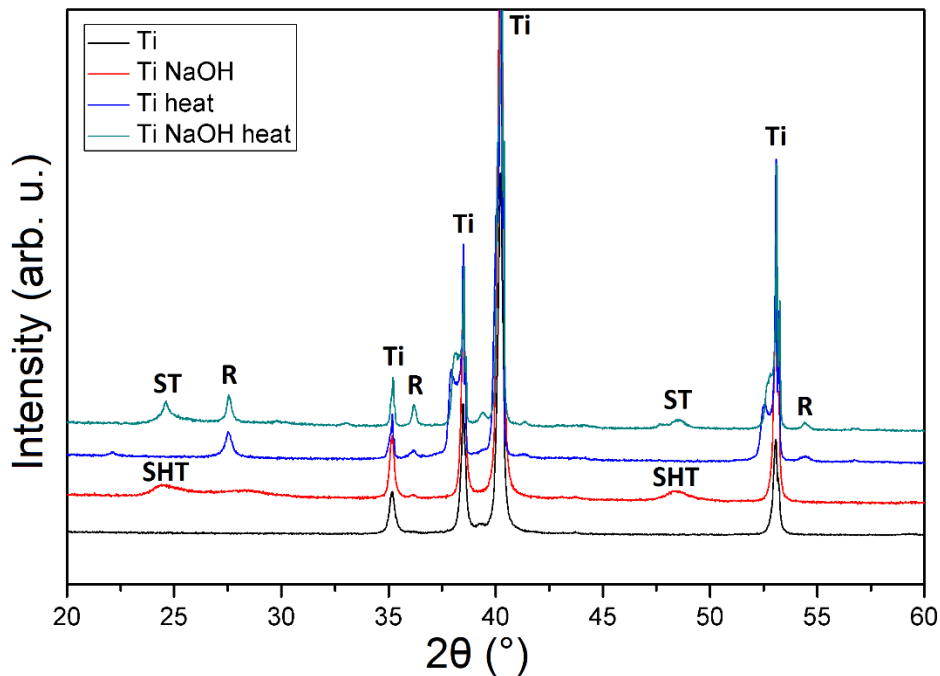

Figure 1. XRD patterns of four surfaces before immersion in SBF. Pure Ti is identified for as-polished titanium. For NaOH treated Ti, poorly crystalline sodium hydrogen titanate (SHT) $Na_{0.8}H_{1.2}Ti_3O_7$ (00-048-0693) can be identified in addition to Ti. Ti and rutile (R) TiO_2 (01-089-4920) are found on heat treated Ti. NaOH and heat treatment results in a mixture of Ti, TiO_2 rutile (01-089-4920), and sodium titanate (ST) $Na_2Ti_6O_{13}$ (00-037-0951). It is possible that Ti_6O (01-072-1807) is also formed on the surface after heat treatments due to the split of the Ti peak at 37°.

Table 4. Summary of HA deposition on four surfaces in different SBFs.

Treatment	Main crystalline phases	BCS-1	BCS-2	c-SBF	BCS-1	BCS-2	c-SBF
			No BSA			1g/L BSA	
--	Ti	—	—	—	—	—	—
Heat	Ti, TiO_2 (rutile)	—	—	—	—	—	—
NaOH	Ti, $Na_{0.8}H_{1.2}Ti_3O_7$	✓	✓	✓	✓	✓	—
NaOH, heat	Ti, TiO_2 (rutile), $Na_2Ti_6O_{13}$	✓	✓	—	✓	—	—

From the XRD patterns, it is found that after the AFA test, as-polished titanium and heat treated titanium did not have apatite on the surface in all three SBFs used, irrespective of the use of proteins. This is also confirmed in SEM, as shown in Figure S3. Nano-crystalline hydroxyapatite (01-074-0565) was identified by XRD on various surfaces as summarized in Table 4. Figure 2 gives an example of the XRD patterns of HA-covered NaOH treated Ti surfaces from all three SBFs without the addition of proteins. However, in the presence of 1g/L BSA, HA formation was strongly inhibited in c-SBF, while HA can still be observed in BCS-1 and BCS-2. In the case of NaOH and heat treated Ti, no HA formation was observed in c-SBF. HA was detected with BCS-1 and BCS-2 without proteins, but only in BCS-1 in the presence of proteins. The surface morphologies are shown in Figure 3. HA was formed on NaOH treated Ti in all three SBFs with larger HA globules found in c-SBF. However, in the case of c-SBF, the HA layer does not fully cover the material as the exposed porous surface layer can still be occasionally observed, as can be seen in Figure 3c. It is difficult to conclude from the final morphologies the precipitation pathways, but these features seem to suggest a lower nucleation rate, which leads to fewer nucleation centers on the surface and a concurrent increase in surface area not covered by HA. In other cases, no obvious morphology differences were found between HA formed in solutions with BSA and solutions without.
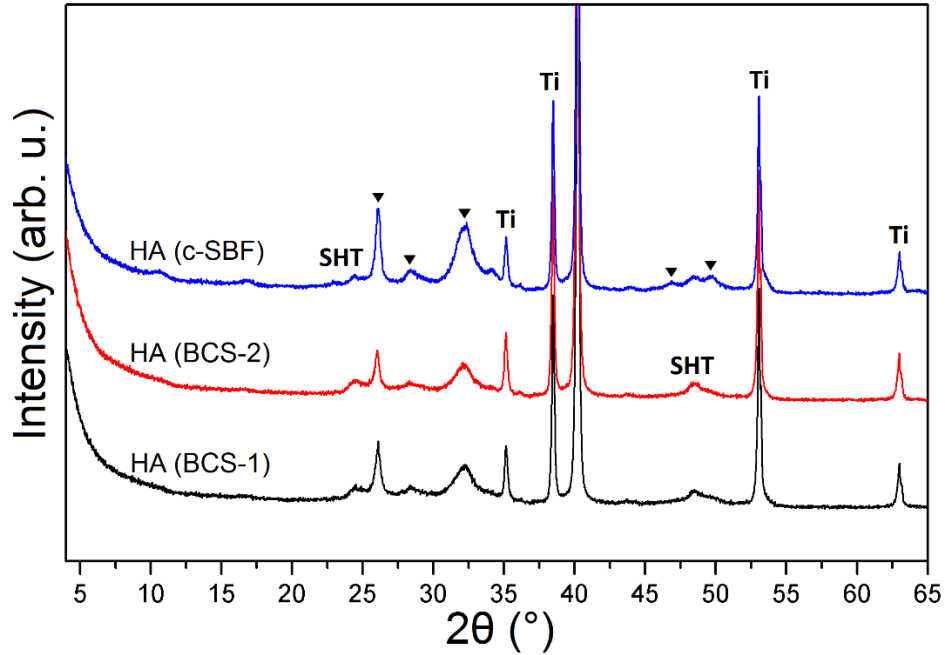
Figure 2. XRD patterns of NaOH treated Ti surfaces after immersion in BCS-1, BCS-2 and c-SBF for one week. Sodium hydrogen titanate (SHT) and titanium (Ti) peaks are indicated and HA peaks are marked with a triangle. In the calcium phosphate family, OCP and HA have similar diffraction patterns at $20° - 45°$ but the absence of peaks at around $5°$ confirmed the formation of HA instead of OCP.
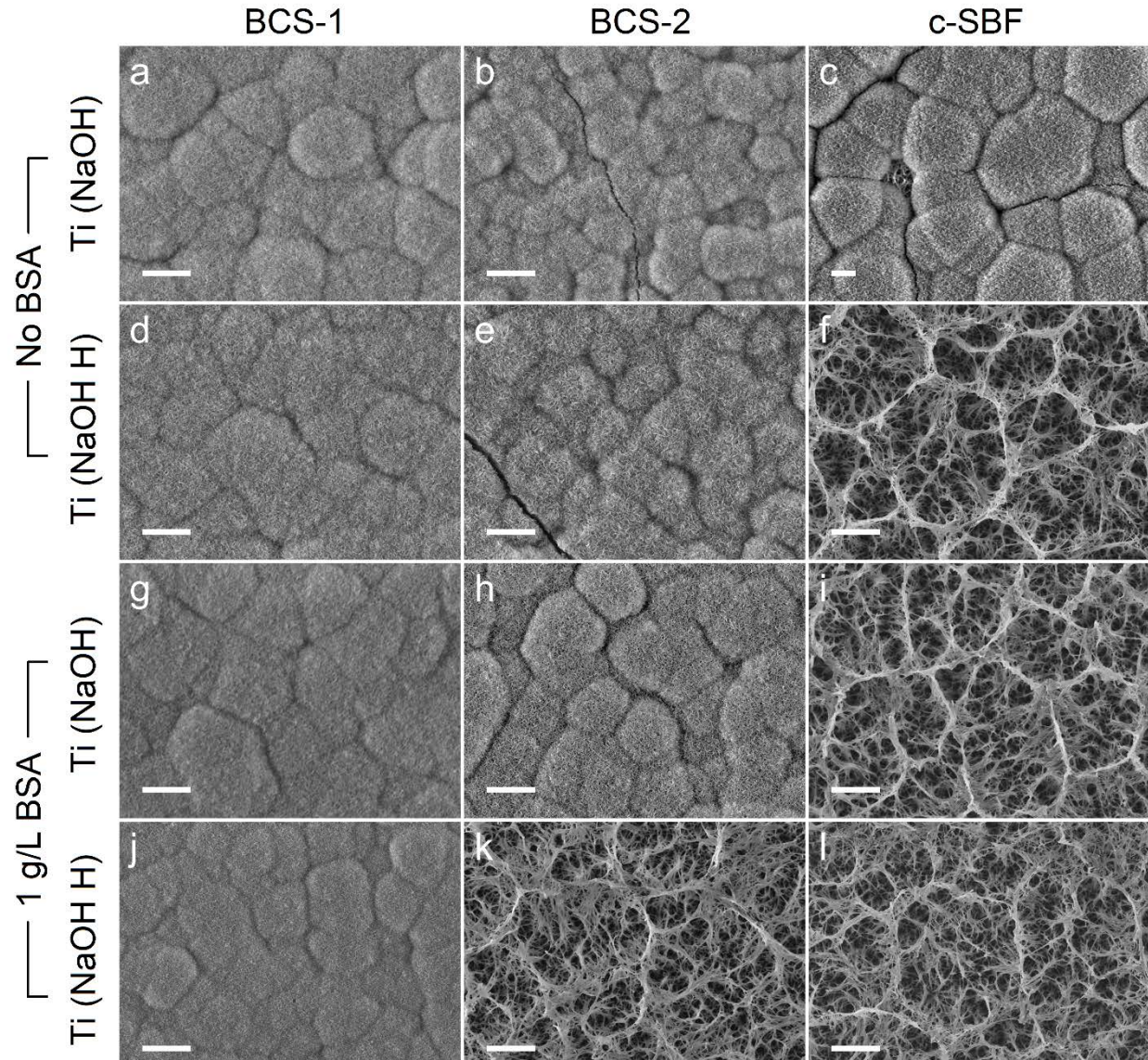
Figure 3. SEM images of surfaces immersed in various SBFs for one week. Three columns from left to right are with BCS-1 (a, d, g, j), BCS-2 (b, e, h, k) and c-SBF (c, f, i, l), respectively. Two top rows are with NaOH treated Ti (a, b, c), NaOH and heat treated Ti (d, e, f) without BSA in SBF. Bottom two rows are the same NaOH treated Ti (g, h, i), NaOH and heat treated Ti (j, k, l) with 1g/L BSA in solution. Apatite formation can be easily identified by the presence of globules consisting of tiny flake-like crystals, the characteristic morphologies of HA deposited from SBF. The presence of porous surface in the case of f, i, k and l indicates no HA deposition. All scale bars are 2 µm.

The current results suggest that NaOH treated Ti has a higher AFA before undergoing a further heat treatment, as expected [12]. At the same time, it also suggests that the three solutions can be ranked based on their ability to form HA on a testing material as BCS-1 > BCS-2 > c-SBF, which agrees with the calculated degrees of supersaturation with respect to HA. The presence of BSA inhibited the HA

nucleation on surfaces, and no promoting effect of the BSA was observed at the current concentration of 1g/L. It is interesting to note that in the presence of proteins, the AFA can still be expressed in the new carbonate-buffered SBFs but not in c-SBF. A general idea of the amount of HA precipitated can be obtained by calculating the area under the HA peak in the XRD patterns, shown in Figure 4. This data however only gives a semi-quantitative estimate as the peak intensity in XRD also depends on the degree of crystallinity. Nevertheless, a general consistency between XRD and SEM results can be observed.
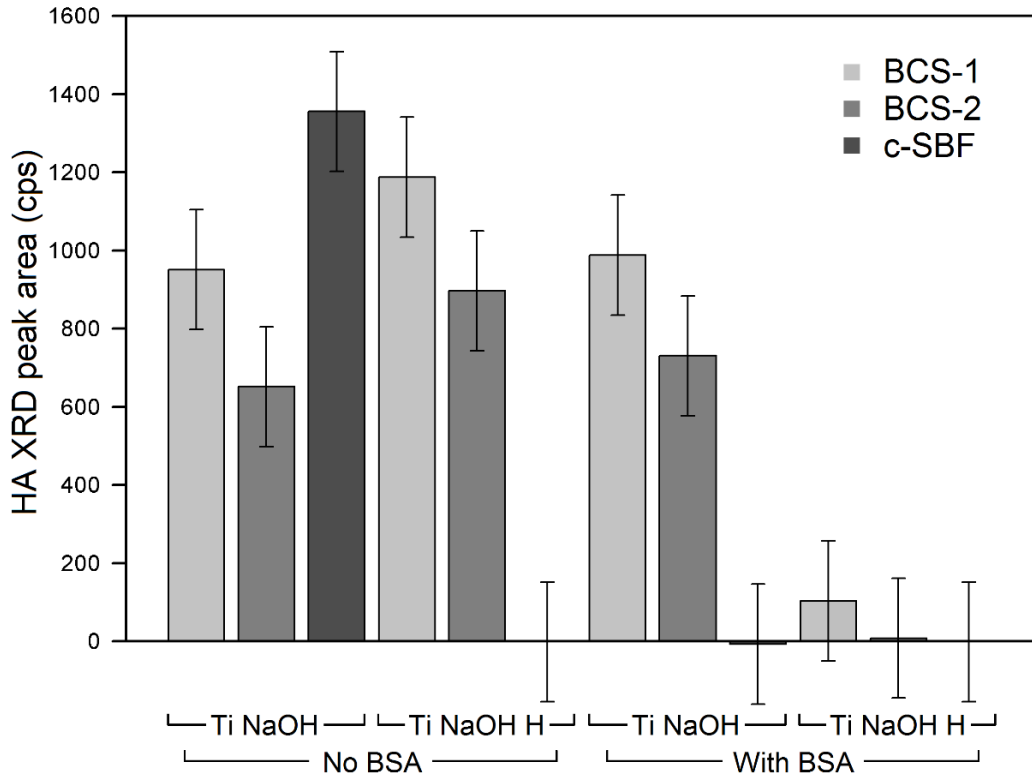
Figure 4. Amounts of HA deposition on various surfaces in different SBFs calculated by area integration under the XRD peak of HA at 25.8°. The error bars correspond to 95% confidence intervals (means of 2 observations).

The composition of the deposited hydroxyapatite can be compared by FTIR. Figure 5 shows a comparison of NaOH treated Ti immersed in BCS-1, BCS-2, c-SBF and BCS-1 with 1g/L BSA. HA precipitated in all these cases as detected in XRD and SEM. A broad phosphate band was found in the region from 1200 to 960 cm^{-1} for all the samples. The phosphate $(PO_4)^{3-}$ also contributes to peaks at 601 and 557 cm^{-1}. The major difference between the samples are the presence of strong bands from carbonate at 1417 and 872 cm^{-1} for HA precipitated from BCS-1 and BCS-2 versus c-SBF, indicating a greater incorporation of carbonate into the apatite structure. This is also expected due to the higher concentrations of carbonates in solution BCS-1 and BCS-2. In the presence of 1g/L BSA, HA still precipitated on NaOH

treated Ti in BCS-1. At the same time, the emergence of two peaks at 1652 and 1538 cm^{-1} indicates the adsorption of BSA on the surface [38].
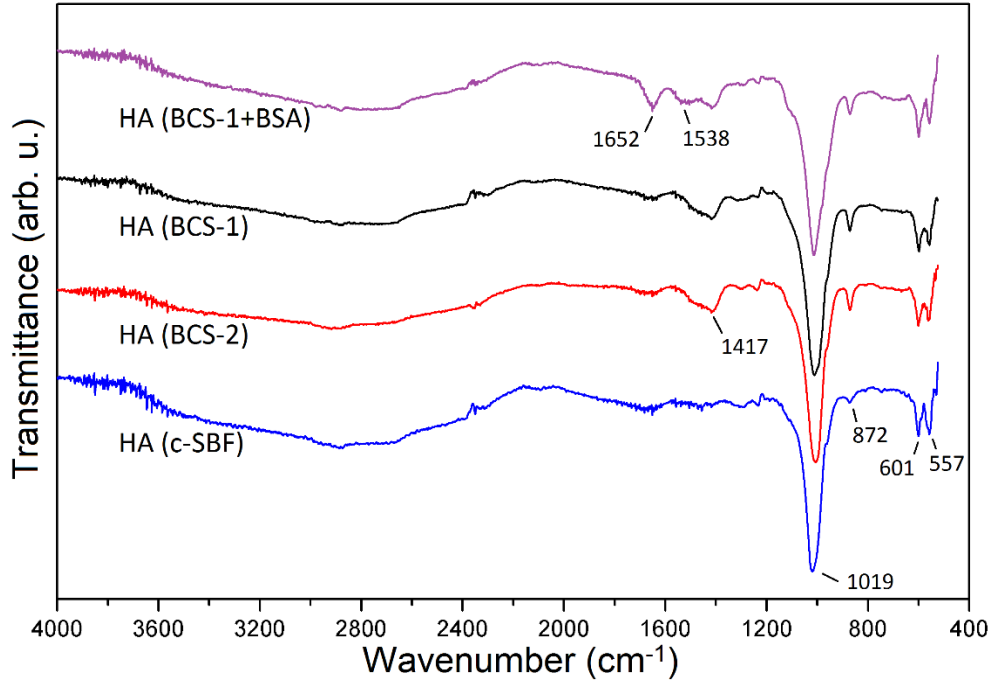
Figure 5. FTIR transmission spectra of NaOH treated Ti after AFA test in different SBFs.

Table 5. Assignments of FTIR bands of NaOH treated Ti immersed in different SBFs.

| Wavenumber [cm^{-1}]	Component	HA (BCS-1)	HA (BCS-2)	HA (c-SBF)	HA (BCS-1+BSA)
1652	BSA				✓
1538	BSA				✓
1417	$(CO_3)^{2-}$	✓	✓		✓
1019	$(PO_4)^{3-}$	✓	✓	✓	✓
872	$(CO_3)^{2-}$	✓	✓	✓	✓
601	$(PO_4)^{3-}$	✓	✓	✓	✓
557	$(PO_4)^{3-}$	✓	✓	✓	✓

3.3 Kinetic study of the effect of BSA at different concentrations

A general inhibitory effect of BSA on HA nucleation was found from the results in the previous section. Further experiments were conducted to investigate the effect of protein concentrations and the growth kinetics of the apatite. NaOH treated Ti was tested in SBF BCS-2 at three different BSA concentrations at 0.1g/L, 1g/L and 5g/L and also in BCS-2 without BSA at three different time delays of 3 days, 7 days and 14 days using individual samples (Table 6).

Table 6. Statistical design of experiments to investigate the effect of BSA concentrations.

Factor	Definition	Levels			
		1	2	3	4
A	Time delay (d)	3	7	14	
B	BSA (g/L)	0	0.1	1	5
C	Replicate	1	2		

XRD results indicate a positive HA deposition from solution without BSA and with BSA at 0.1g/L and 1g/L at all three time points, but a total inhibition of HA formation at 5g/L, even after two weeks. A comparison of surfaces tested with 1g/L BSA and 5g/L BSA is given in Figure 6. The results from XRD are supported by observations in SEM, shown in Figure S4. The calcium phosphate deposited from the SBF was quantified using ICP measurements of the remaining solution and is presented in Figure 7. The results reveal that a BSA concentration of 0.1g/L have little effect on the amount of HA growth on NaOH treated Ti, whereas a BSA concentration of 1g/L seems to slow down the initial HA growth at 3 days but does not seem to have an effect on the HA growth afterwards. The effect of BSA becomes significant when the concentration of BSA reaches 5 g/L, where a total inhibition of HA formation takes place.
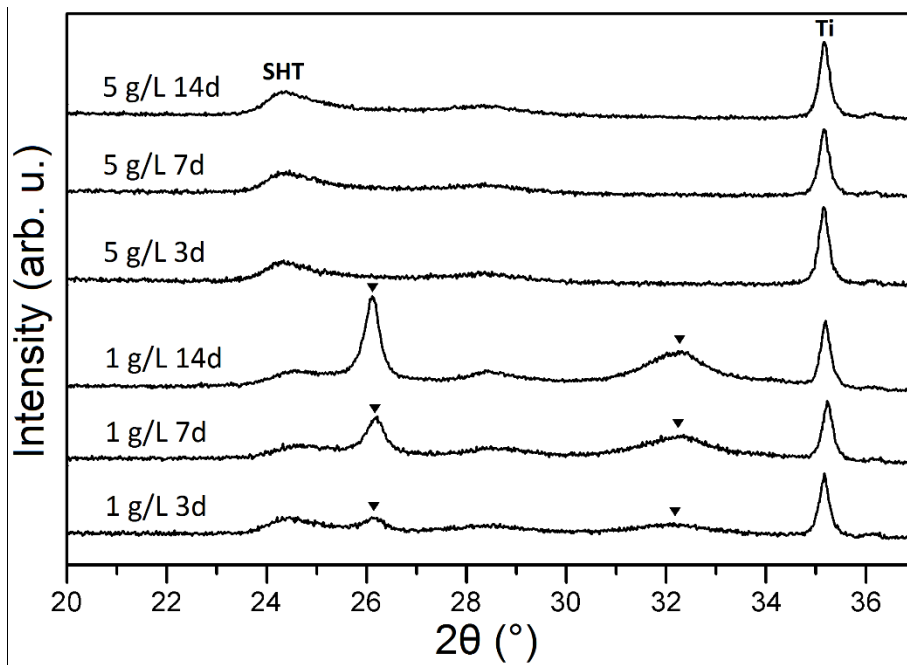
Figure 6. XRD patterns of NaOH treated Ti in BCS-2 with 1g/L and 5g/L BSA at three different time delays. The titanium (Ti) and sodium hydrogen titanate (SHT) are marked and the HA peaks are labelled with triangles.
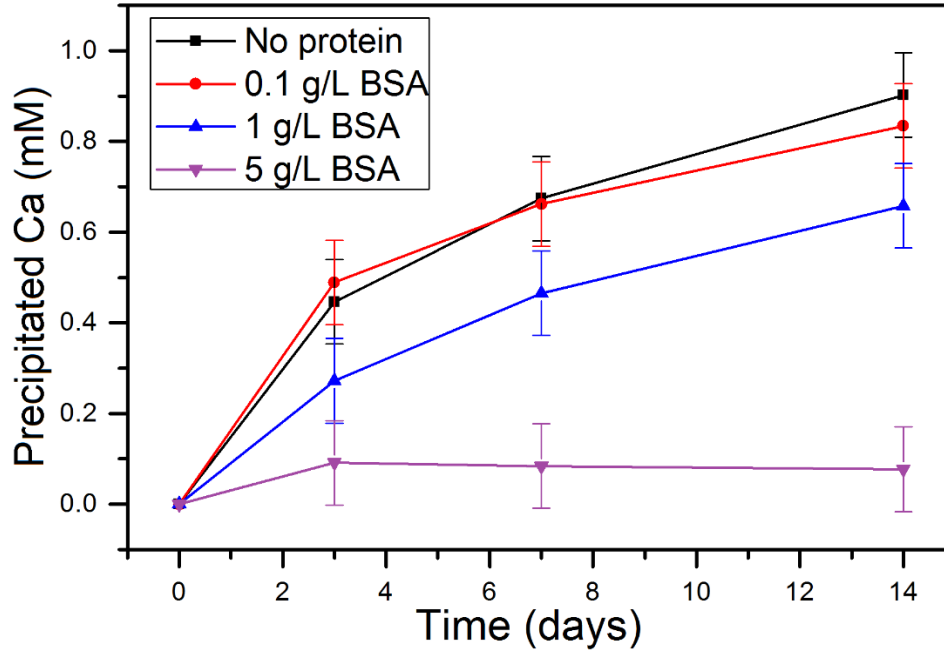
Figure 7. Quantitative kinetic study of HA growth on NaOH treated Ti in BCS-2 with different protein concentrations. The graph is based on the fitted values using statistical analysis on the original data adopting a type I error risk of 5%. The plot of raw data is given in supplementary information Figure S5.

3.4 Effect of BSA on solution pH and free calcium concentration

The presence of BSA raises questions in terms of the amount of free calcium ions available in the solution, as it is known that proteins can bind Ca^{2+} ions [16], affecting the degree of supersaturation. The measurements of free calcium ion were conducted in calcium solutions with different BSA concentrations ranging from 0 – 20 g/L in a solution buffered with Tris-HCl. The pH of the solution without BSA was measured to be 7.44 ($\pm$ 0.02). With 20 g/L BSA, the pH measured is 7.36 ($\pm$ 0.01), slightly lower compared to the previous value as BSA is known to be acidic in aqueous conditions [16]. Figure 8 gives the plot of the change of available free calcium ions as a function of BSA concentration. A good linear fit can be obtained with data points collected of solutions containing BSA, showing a decrease of free Ca concentration with the addition of BSA. However, the first data point at 0 g/L BSA is an adjusted value using the linear extrapolation due to possible different electrode responses (raw data given in Table S3). Although a 20 g/L BSA solution would reduce the free Ca^{2+} by roughly 13%, a 5g/L BSA only reduces the free Ca^{2+} by about 3%, which would decrease the $\log(S_{HA})$ value by less than 0.1 according to calculations. This suggests that the strong inhibitory effect of proteins is unlikely a result of the decrease of available free Ca^{2+} ions in SBFs.
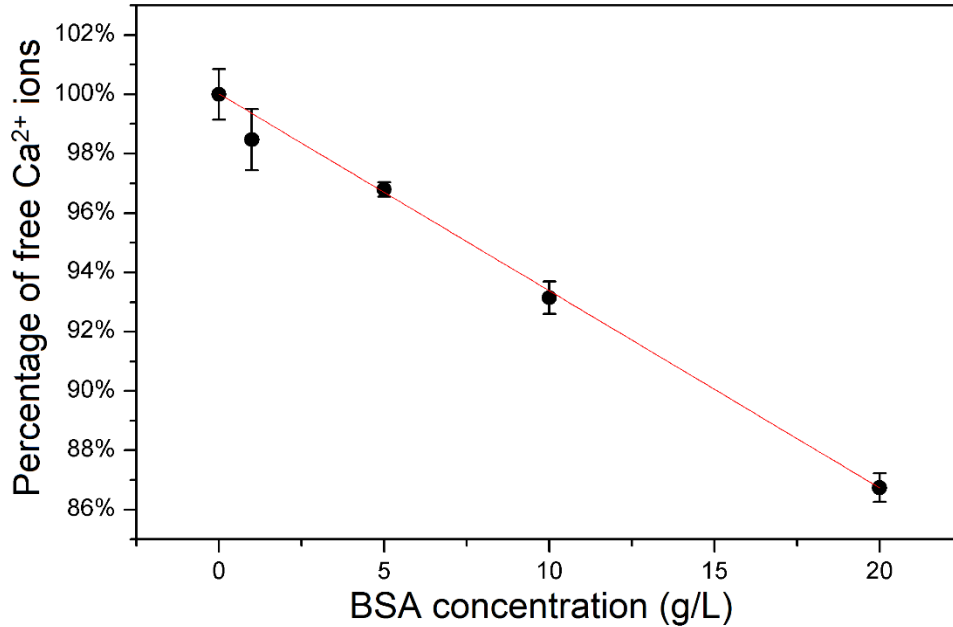
Figure 8. Plot of free calcium ion concentration with different BSA concentrations. Data were normalized to the free calcium in solution without BSA. A linear fit of the data obtained with the presence of BSA gives: $y = 1.000 - 0.007 \cdot x$, $R^2 = 0.996$.

The proposed BCS-1 and BCS-2 were buffered with carbonates so the effect of BSA on solution pH was investigated separately. The pH values were obtained with 1g/L and 5g/L BSA in two solutions under testing conditions (36.5°C, $p(CO_2) = 5\%$), and compared with the solution pH without the presence of proteins (Figure 9). For both solutions, a slight decreasing trend of pH with BSA concentration can be observed, but the pH values remain close with lowest pH being around 7.36. A thermodynamic calculation indicates only a slight change in the degree of supersaturation of HA, from 10.89 to 10.74 for BCS-1 and from 10.63 to 10.47 for BCS-2. These results indicate that the inhibitory effect of BSA on HA nucleation is also unlikely to be due to the change in solution pH.
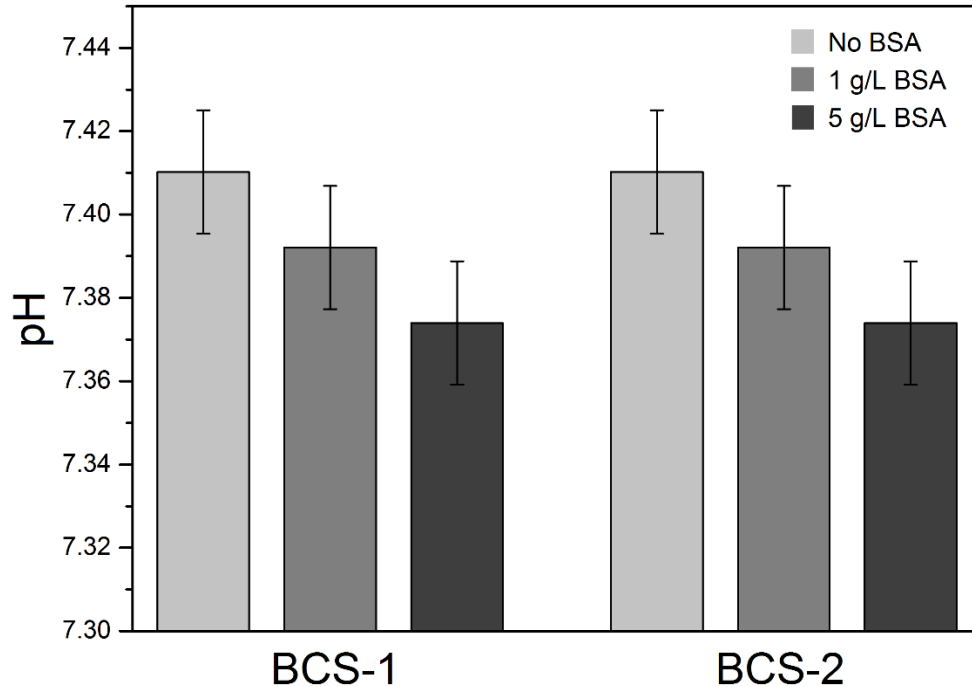
Figure 9. pH values measured of BCS-1 and BCS-2 without BSA and in the presence of BSA at 1 g/L and 5 g/L. The column chart is based on the fitted values using statistical analysis on the original data adopting a type I error risk of 5%. Only the factor of protein concentration was shown to be significant ($p < 0.001$). The plot of raw data is given in supplementary information Figure S6.

4. Discussion

Requirements of solutions as simulated body fluids

The ability to trigger the formation of apatite from an SBF is used to imply the bioactivity of an implant *in vivo*. To be used as an SBF, the proposed solution should meet several requirements. i) The solution should have a pH value close to the physiological pH at around 7.40 and possess reasonable buffering capacity to maintain its pH. The proposed BCS-1 and BCS-2 were designed to have a target pH of 7.40 under conditions in AFA test, which was verified experimentally. The pH is buffered with carbonates in equilibrium with a controlled 5% CO_2 environment in an incubator. The pH buffering capacity can also be calculated theoretically and is slightly better than c-SBF, shown in Figure S7. ii) The solution should not precipitate HA in the absence of the testing materials. Since SBF is supersaturated with respect to HA, theoretically no SBF will be stable indefinitely. However, it is necessary to be stable at least during the recommended testing time to avoid homogenous nucleation of HA in the solution, which could lead to false positive results. The stability of the solution BCS-1 and BCS-2 was investigated and confirmed for a

period of 4 weeks. Details about the methodology and the results are presented in the supporting information (SI–8). iii) The solution should deliver expected results on both negative and positive controls, namely not to have HA nucleation on materials that have been proven to be inert *in vivo* but to deposit HA on materials with *in vivo* bioactivity. Previous animal experiments have confirmed that as-polished Ti being an inert material while NaOH treatment could induce bioactivity of Ti [13][34]. The results of the present work also show that the two proposed SBFs do not show HA deposition on as-polished Ti but instead on NaOH treated Ti, satisfying this requirement.

Comparison of SBFs and the role of carbonates

The major difference between the proposed SBF and the c-SBF is the carbonate concentration. Higher amount of carbonates can be used to buffer solution pH under equilibrium with 5% CO_2 but also leads to potential storage issues. In ambient conditions with 0.04% CO_2 in air, the carbonated solution could easily lose CO_2 and result in a pH value higher than 7.40, eventually leading to a homogenous nucleation of HA in solution (instability). Our effort in preventing undesired homogenous nucleation was to separate the calcium and phosphate components into two stock solutions and mix them uniformly before the AFA test. Still, care should be taken with solution A due to the same reason. For the use of c-SBF, the effect of carbonates is however overlooked in the ISO protocols. The current lower carbonate concentration (4.2 mM HCO_3^-) in c-SBF is a result of instability of SBFs with higher carbonate content which leads to calcite formation [39]. In fact, even in the current concentration at 4.2 mM, the calculated partial pressure of CO_2 in c-SBF is still much higher than that in air (1.0% vs. 0.04%), meaning it will gradually release CO_2 from the solution and result in a higher pH value. In the current study, 1 mL 1M HCl (for 1L of SBF) was added to balance the solution pH (Step 6 in ISO protocol). A calculation shows that depending on the degree of CO_2 exchange with air, the pH can vary from 7.34 – 7.51. This is likely the reason why a range (from 0 to 5 mL) of 1M HCl is given in the ISO protocol to adjust the final pH value to 7.40. The issue of carbonate loss and slight change of pH during preparation and storage of the c-SBF is in general not taken into account. Although at the time of preparation the solution pH is adjusted to 7.40, during the storage and the use, the slight carbonate loss would still increase the pH and thus the supersaturation of the solution, which could potentially lead to inconsistent results from following this protocol. A detailed analysis is given in SI–9. A fixed volume of additional HCl and the awareness of possible carbonate exchange is recommended for the use of c-SBF.

Possible causes of the inhibitory effect of BSA

In this study, the inhibitory effect of BSA on the nucleation of HA has been observed in all three SBFs used. As the possible complexation effect with free Ca^{2+} ions was previously reported [40], we investigated the decrease of free Ca^{2+} ions by proteins using a calcium-selective electrode. A small decrease in free calcium ions (~3% at 5g/L BSA) was found, which by itself can hardly explain a complete inhibition of HA formation. The effect of pH change has also been confirmed to have a negligible effect on supersaturation and hence HA nucleation and growth. On the other hand, protein adsorption on surfaces is a common phenomenon. The adsorption of proteins onto implant surfaces would serve as a competitive event for adsorption of inorganic species such as Ca^{2+}, PO_4^{3-} or HPO_4^{2-}, thus affecting the nucleation of calcium phosphates. Recently, non-classical nucleation theory has been proposed for several calcium systems and pre-nucleation clusters in the system of Ca-P has been observed [41][42][43]. Although the active nucleation species in the SBF under discussion here remain unknown, proteins might have a stabilization effect on the pre-nucleation clusters, thus affecting the nucleation event. Currently, efforts are also being made to approach the problem from a fundamental perspective using atomistic simulations, such as the competitive adsorption of organic materials with inorganic ions onto model surfaces such as rutile.

Possible improvement of the current AFA protocol

Potential ways to improve the use of SBFs in implant evaluation can be suggested from our study. Essentially, the formation of HA from SBF is a heterogeneous nucleation process. Different materials have different abilities to trigger HA deposition *in vivo* or *in vitro*. At the same time, different SBFs also have different tendencies to deposit HA on the same material. Assuming the HA layer formed *in vivo* has a promoting effect on bone growth and bonding, then the question is to find an SBF with the right degree of supersaturation with respect to HA to distinguish materials able to trigger HA deposition *in vivo* from materials which cannot. A simple mimic of blood plasma based on total ion concentrations however cannot guarantee complete successful predictions, considering the obvious differences between the implantation environments in human bone defects versus a solution with solely inorganic ions. However, tuning of the supersaturation levels of the solution can get us closer to better predictions. At the same time, the experimental details including the handling of SBFs (control of carbonate loss), the renewal of solution in long-term studies, or the presence of confined space in SBF, all could have an equally important role in determining the final outcome [35]. Standardization of the operating procedures with a finer control of experimental details is needed to reduce the number of conflicting results in the field

generated using different SBF compositions and different experimental conditions. Understanding the complexity and the subtleties of the system is crucial in understanding and interpreting the results produced using SBFs.

With the knowledge of the inhibitory effect of BSA on HA nucleation, it is recommended to consider adding proteins into the SBF, not because it would decrease the ability to form HA, which could be compensated by adding more inorganic ions, but because of its possible specific interactions with certain materials especially porous materials, thus having different inhibitory behaviors on different materials. In the current study, it seems that in the presence of proteins, carbonate-buffered SBFs, compared to c-SBF, can still generate results that corresponds to the conclusions from *in vivo* experiments, where proteins are in abundance.

Despite limitations of the *in vitro* SBF method, and the emergence of new functional materials with specific cell interactions, which no longer rely on calcium phosphate formation to achieve bioactivity, the authors still consider the method of using SBFs as an *in vitro* method to be a significant contribution to the field of implant research, serving as a first screening step for potential implants, especially Ti-based materials. Possible improvements of the current method would be beneficial.

5. Conclusions and outlook

The current study compared commonly used c-SBF with carbonate-buffered BCS-1 and BCS-2 containing higher concentration of carbonates. All the solutions were able to distinguish bioactive NaOH-treated Ti and inert as-polished Ti in the AFA test. The presence of BSA in SBF has an inhibitory effect on the nucleation of HA on bioactive surfaces. In the case of NaOH treated Ti, no HA can be observed with 1g/L BSA in Kokubo's c-SBF with a Tris-HCl buffer. However, HA can still be detected in the new carbonate-buffered BCS-1 and BCS-2. For NaOH and heat treated Ti, no HA was found with c-SBF irrespective of the addition of BSA but can be found when using BCS-1 and BCS-2 without BSA. Further addition of BSA exhibited a strong inhibitory effect with only BCS-1 being able to produce HA, indicating a higher ability to precipitate HA in the presence of proteins. Using NaOH treated Ti, the effect of BSA was further confirmed to be concentration dependent with minor effect at 0.1g/L and 1g/L but a full inhibition when the concentration reached 5g/L. The measurements of solution pH and free calcium concentration changes due to BSA suggest that the inhibitory effect is not likely to be a result of the decrease of pH or free calcium ions in SBFs.

Proteins were found to have a profound effect on HA nucleation at a concentration much lower than that in human blood plasma. Consequently, the inclusion of proteins in SBFs should receive more attention in future research. Particularly, it would be interesting to identify proteins in human blood plasma that are the key players in controlling the HA nucleation. The complexity of the system calls for the use of statistical design of experiments to identify key parameters and their possible interplay. In the end, the ability for accurate prediction of *in vivo* results of any proposed SBF should be validated by animal experiments. This is currently under investigation and will be reported in the near future.

Acknowledgements

References

[1]   W.C.A. and T.K.G. L. L. Hench, R. J. Splinter, Bonding mechanisms at the interface of ceramic prosthetic materials, J. Biomed. Mater. Res. 5 (1971) 117–141.

[2]   J.R. Jones, Review of bioactive glass: From Hench to hybrids, Acta Biomater. 9 (2013) 4457–4486. doi:10.1016/j.actbio.2015.07.019.

[3]   T. Kokubo, H. Kushitani, S. Sakka, T. Kitsugi, T. Yamamum, Solutions able to reproduce in vivo surface-structure changes in bioactive glass-ceramic A-W, J. Biomed. Mater. Res. 24 (1990) 721–734.

[4]   T. Kokubo, H. Takadama, How useful is SBF in predicting in vivo bone bioactivity?, Biomaterials. 27 (2006) 2907–2915. doi:10.1016/j.biomaterials.2006.01.017.

[5]   T. Kokubo, Surface chemistry of bioactive glass-ceramics, J. Non. Cryst. Solids. 120 (1990) 138–151.

[6]   T. Kokubo, H.M. Kim, M. Kawashita, T. Nakamura, Bioactive metals: Preparation and properties, J. Mater. Sci. Mater. Med. 15 (2004) 99–107.

[7]   T. Kokubo, S. Yamaguchi, Novel bioactive titanate layers formed on Ti metal and its alloys by chemical treatments, Materials (Basel). 3 (2010) 48–63. doi:10.3390/ma3010048.

[8]   T. Kokubo, Implants for surgery - In vitro evaluation for apatite-forming ability of implant materials, ISO 23317:2014, 2014.

[9]   P. Tambasco De Oliveira, A. Nanci, Nanotexturing of titanium-based surfaces upregulates expression of bone sialoprotein and osteopontin by cultured osteogenic cells, Biomaterials. 25

(2004) 403–413. doi:10.1016/S0142-9612(03)00539-8.

[10]   T. Kaito, A. Myoui, K. Takaoka, N. Saito, M. Nishikawa, N. Tamai, H. Ohgushi, H. Yoshikawa, Potentiation of the activity of bone morphogenetic protein-2 in bone regeneration by a PLA-PEG/hydroxyapatite composite, Biomaterials. 26 (2005) 73–79. doi:10.1016/j.biomaterials.2004.02.010.

[11]   A.A. Zadpoor, Relationship between in vitro apatite-forming ability measured using simulated body fluid and in vivo bioactivity of biomaterials, Mater. Sci. Eng. C. 35 (2014) 134–143. doi:10.1016/j.msec.2013.10.026.

[12]   H.M. Kim, F. Miyaji, T. Kokubo, T. Nakamura, Effect of heat treatment on apatite-forming ability of Ti metal induced by alkali treatment, J. Mater. Sci. Mater. Med. 8 (1997) 341–347.

[13]   S. Nishiguchi, T. Nakamura, M. Kobayashi, H.M. Kim, F. Miyaji, T. Kokubo, The effect of heat treatment on bone-bonding ability of alkali-treated titanium, Biomaterials. 20 (1999) 491–500. doi:10.1016/S0142-9612(98)90203-4.

[14]   L. Sava, S. Pillai, U. More, A. Sontakke, Serum calcium measurement: Total versus free (ionized) calcium., Indian J. Clin. Biochem. 20 (2005) 158–161. doi:10.1007/BF02867418.

[15]   M. Bohner, J. Lemaitre, Can bioactivity be tested in vitro with SBF solution?, Biomaterials. 30 (2009) 2175–9. doi:10.1016/j.biomaterials.2009.01.008.

[16]   J.E. Ellingsen, A study on the mechanism of protein adsorption to TiO2, Biomaterials. 12 (1991) 593–596.

[17]   V. Hlady, H. Füredi-Milhofer, Adsorption of human serum albumin on precipitated hydroxyapatite, J. Colloid Interface Sci. 69 (1979) 460–468. doi:10.1016/0021-9797(79)90135-8.

[18]   J. Garnett, P. Dieppe, The effects of serum and human albumin on calcium hydroxyapatite crystal growth., Biochem. J. 266 (1990) 863–868.

[19]   D.T.H.W.G. Embery, Adsorption of bovine serum albumin on to titanium powder, Biomaterials. 17 (1996) 859–864. doi:10.1016/0006-3002(56)90469-3.

[20]   V. Vergaro, C. Carlucci, M. Cascione, C. Lorusso, F. Conciauro, B.F. Scremin, P.M. Congedo, G. Cannazza, C. Citti, G. Ciccarella, Interaction between Human Serum Albumin and Different Anatase TiO 2 Nanoparticles : A Nano-bio Interface Study Regular Paper, Nanomater. Nanotechnol. 5 (2015) 1–12. doi:10.5772/61092.

[21]   S. Mann, D.D. Archibald, J.M. Didymus, T. Douglas, B.R. Heywood, F.C. Meldrum, N.J. Reeves, Crystallization at Inorganic-Organic Interfaces: Biominerals and Biomimetic Synthesis, Science (80-.). 261 (1993) 1286–1292.

[22]   H. Pan, X. Zhao, B.W. Darvell, W.W. Lu, Apatite-formation ability - Predictor of "bioactivity"?, Acta Biomater. 6 (2010) 4181–4188. doi:10.1016/j.actbio.2010.05.013.

[23]   A. Lussi, M.A. Crenshaw, A. Linde, Induction and inhibition of hydroxyapatite formation by rat dentine phosphoprotein in vitro, Arch. Oral Biol. 33 (1988) 685–691. doi:10.1016/0003-9969(88)90124-0.

[24]   V. Stenport, P. Kjellin, M. Andersson, F. Currie, Y.-T. Sul, a Wennerberg, a Arvidsson, Precipitation of calcium phosphate in the presence of albumin on titanium implants with four different possibly bioactive surface preparations. An in vitro study., J. Mater. Sci. Mater. Med. 19 (2008) 3497–505. doi:10.1007/s10856-008-3517-z.

[25]   A. Arvidsson, F. Currie, P. Kjellin, Y.-T. Sul, V. Stenport, Nucleation and growth of calcium phosphates in the presence of fibrinogen on titanium implants with four potentially bioactive surface preparations. An in vitro study., J. Mater. Sci. Mater. Med. 20 (2009) 1869–79. doi:10.1007/s10856-009-3755-8.

[26]   M.T. Jahromi, G. Yao, M. Cerruti, The importance of amino acid interactions in the crystallization of hydroxyapatite., J. R. Soc. Interface. 10 (2013) 20120906. doi:10.1098/rsif.2012.0906.

[27]   J.. L.. Gamble, J. Lawder, Chemical anatomy , physiology and pathology of extracellular fluid : a lecture syllabus, Harvard Medical School, 1941.

[28]   L. Muller, F.A. Muller, Preparation of SBF with different HCO3 content and its influence on the composition of biomimetic apatites, Acta Biomater. 2 (2006) 181–189. doi:10.1016/j.actbio.2005.11.001.

[29]   Q.J. He, Z.L. Huang, X.K. Cheng, J. Yu, Thermal stability of porous A-type carbonated hydroxyapatite spheres, Mater. Lett. 62 (2008) 539–542. doi:10.1016/j.matlet.2007.06.001.

[30]   E. Landi, G. Celotti, G. Logroscino, a. Tampieri, Carbonated hydroxyapatite as bone substitute, J. Eur. Ceram. Soc. 23 (2003) 2931–2937. doi:10.1016/S0955-2219(03)00304-2.

[31]   C. Rey, B. Collins, T. Goehl, I.R. Dickson, M.J. Glimcher, The carbonate environment in bone mineral: A resolution-enhanced fourier transform infrared spectroscopy study, Calcif. Tissue Int. 45 (1989) 157–164. doi:10.1007/BF02556059.

[32]   H. Pan, B.W. Darvell, Effect of carbonate on hydroxyapatite Solubility, Cryst. Growth Des. 10 (2010) 845–850. doi:10.1021/cg901199h.

[33]   D.C. Montgomery, Design and Analysis of Experiments, 5th Edition, Wiley, 2000. doi:978-0-470-56319-9.

[34]   S. Nishiguchi, H. Kato, H. Fujita, M. Oka, H.M. Kim, T. Kokubo, T. Nakamura, Titanium metals form direct bonding to bone after alkali and heat treatments, Biomaterials. 22 (2001) 2525–2533.

[35]   X.-X. Wang, W. Yan, S. Hayakawa, K. Tsuru, A. Osaka, Apatite deposition on thermally and anodically oxidized titanium surfaces in a simulated body fluid, Biomaterials. 24 (2003) 4631–4637. doi:10.1016/S0142-9612(03)00357-0.

[36] S. Yamaguchi, H. Takadama, T. Matsushita, T. Nakamura, T. Kokubo, Cross-sectional analysis of the surface ceramic layer developed on Ti metal by NaOH-heat treatment and soaking in SBF, J. Ceram. Soc. Japan. 117 (2009) 1126–1130. doi:10.2109/jcersj2.117.1126.

[37] T. Kokubo, S. Yamaguchi, Bioactive Ti metal and its alloys prepared by chemical treatments: State-of-the-art and future trends, Adv. Eng. Mater. 12 (2010) 579–591. doi:10.1002/adem.201080087.

[38] J. Grdadolnik, Y. Maréchal, Bovine serum albumin observed by infrared spectrometry. I. Methodology, structural investigation, and water uptake., Biopolymers. 62 (2001) 40–53. doi:10.1002/1097-0282(2001)62:1<40::AID-BIP60>3.0.CO;2-C.

[39] A. Oyane, H.-M. Kim, T. Furuya, T. Kokubo, T. Miyazaki, T. Nakamura, Preparation and assessment of revised simulated body fluids., J. Biomed. Mater. Res. A. 65 (2003) 188–195.

[40] J. Lima, S.R. Sousa, A. Ferreira, M.A. Barbosa, Interactions between calcium phosphate and albumin on the surface of titanium, J. Biomed. Mater. Res. 55 (2000) 45–53. doi:Doi 10.1002/1097-4636(200104)55:1<45::Aid-Jbm70>3.0.Co;2-0.

[41] J.J. De Yoreo, P.U.P.A. Gilbert, N.A.J.M. Sommerdijk, R.L. Penn, S. Whitelam, D. Joester, H. Zhang, J.D. Rimer, A. Navrotsky, J.F. Banfield, A.F. Wallace, F.M. Michel, F.C. Meldrum, H. Colfen, P.M. Dove, Crystallization by particle attachment in synthetic, biogenic, and geologic environments, Science (80-.). 349 (2015) aaa6760. doi:10.1126/science.aaa6760.

[42] A.K. Bertram, T. Koop, L.T. Molina, M.J. Molina, Clustering of Calcium Phosphate in the System CaCl2-H3PO4-KCl-H2O, J. Phys. Chem. B. Phys. Chem. B. 103 (1999) 8230–8235.

[43] W.J.E.M. Habraken, J. Tao, L.J. Brylka, H. Friedrich, L. Bertinetti, A.S. Schenk, A. Verch, V. Dmitrovic, P.H.H. Bomans, P.M. Frederik, J. Laven, P. van der Schoot, B. Aichmayer, G. de With, J.J. DeYoreo, N.A.J.M. Sommerdijk, Ion-association complexes unite classical and non-classical theories for the biomimetic nucleation of calcium phosphate, Nat. Commun. 4 (2013) 1507. doi:10.1038/ncomms2490.

Electronic Supplementary Information

A comparative study of simulated body fluids in the presence of proteins

Weitian Zhao, Jacques Lemaître and Paul Bowen

Powder Technology Laboratory, Institute of Materials, École Polytechnique Fédérale de Lausanne (EPFL), CH-1015 Lausanne, Switzerland

1. Thermodynamic model

The thermodynamic model is based on a reported model with updated thermodynamic data [1]. In short, calculations are performed based on the material balance equations and the thermodynamic equilibria applied to dissolution and complex formation reactions. The activity coefficients of the ionic species are calculated using the extended Debye-Hückel formula [2],

$$-log\gamma_X = \frac{Az_X^2\sqrt{I}}{1 + Ba_X\sqrt{I}}$$

where Z_X is the charge of the dissolved species X. I is the ionic strength of the solution, defined by

$$I = \frac{1}{2}\sum_X z_X^2[X]$$

[X] is the concentration of species X;
a_X(nm) is the radius of the species X;
A and B are two constants given by the formulas:

$A = 1.8246 \cdot 10^6 \times (\varepsilon T)^{3/2}$ [$L^{1/2} \times K^{3/2} \times mole^{-3/2}$]
$B = 502.9 \times (\varepsilon T)^{1/2}$ [$nm^{-1} \times L^{1/2} \times K^{1/2} \times mole^{-1/2}$]

ε is the dielectric constant of the solvent calculated by the formula:

$\varepsilon = 251.629 - 0.803T + 0.000744T^2$

T [K] is the absolute temperature.

The solver function of Microsoft Excel is used to iteratively solve the activities of the reference ions (namely: Na^+, K^+, Mg^{2+}, Ca^{2+}, HPO_4^{2-}, CO_3^{2-}, SO_4^{2-}, Cl^-...) until selected constraints are met, such as the analytical concentrations of dissolved elements and the equilibrium of selected dissolution reactions etc.

2. Protocols of using SBF-BCS for apatite forming ability test

Preparation of AFA solutions

1. Certain amount of commercial chemicals (Table S1) are added into Milli-Q water in a volumetric flask to make 0.5 L each of solution A and B.
2. The pH of both solution A and solution B should be recorded.

3. Solutions A and B are recommended to be filtered by 0.2 µm syringe filters before use.
4. HDPE (High-Density Polyethylene) bottles can be used for storage of solutions. Air should be minimized for solution A and the bottle be tightly capped. Bottles need to be labeled with the preparation date.
5. Once the bottles are opened, it is not recommended to use solution A afterwards.

<u>Preparation of samples for testing</u>

1. Samples of different shapes can be used, but both surfaces of the samples should be polished and treated.
   a. Samples of rectangular shape can be put in the bottom of the testing tube (Figure S1a).
   b. Samples in the form of discs are recommended to be suspended in the tube to prevent the formation of a closed space under the sample (Figure S1b). Stainless steel hooks can be used to suspend the sample discs.
2. Exchange of CO_2 with the incubator should be allowed during the test, which can be done by opening a hole on the cap of the plastic tube, as in Figure S1.

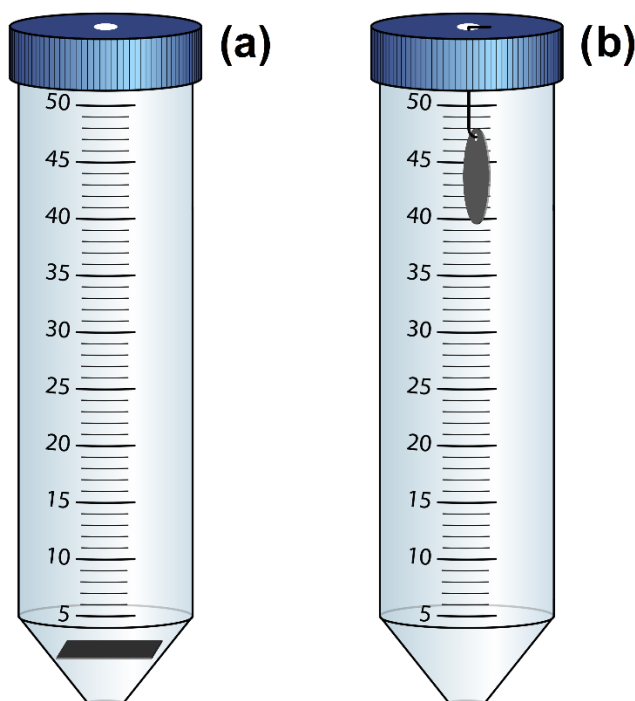<u>Apatite forming ability test</u>

1. All the experimental preparations are recommended to be done in laminar flow hood to avoid dusts which may act as heterogeneous surfaces for nucleation.
2. Proteins, if used, should be put in solution B, together with 0.4g/L NaN_3 (final concentration in SBF at 0.2g/L) to prevent bacterial proliferation.
3. Solution A and B are withdrawn separately by hand-made 30 mL twinned syringe labeled with A and B.
4. Syringes are connected with a Y-connector to an 8-element Kenics static mixer (Figure S2).
5. Solutions are mixed by pushing twin-syringes slowly in a few seconds. Taking care to make sure that equal volumes of A and B are expelled. Gas in the Y connector should be eliminated and only the steady flow of mixture of solution A and B should be collected. An automated system could also be used to mix the two solutions.
6. After sample immersion, the tubes containing the sample and SBF should be quickly transferred into the incubator (ideally within 15 min after mixing of two solutions) to prevent pre-nucleation of any calcium phosphates.
7. The pH of the mixed solution, time delay of measurement and room temperature should be recorded.
8. The presence of proteins especially at high concentrations might affect the stability of the solution. It is recommended to introduce control solutions without testing samples to confirm the stability of the solution for a certain test, or to test the solution stability before the planned experiments, especially studies that last longer than one week.
9. The solution to sample surface ratio should be kept around $V_S = 100 \cdot S_a$ [mm]. Avoid any confined solution volume during the AFA test.
10. Since the solutions are exposed to the environment in incubator, a water reservoir should be placed inside in order to maintain a high relative humidity (> 95%) to prevent drying of SBFs.

Table S1. Preparation of simulated body fluid (SBFs).

Reagent	Purity	BCS-1		BCS-2		Unit
		Solution A	Solution B	Solution A	Solution B	
NaCl	99.5%	6.873	6.873	6.837	6.837	[g/L]
NaHCO$_3$	99.5%	3.749		3.816		[g/L]
KCl	99.5%			0.749		[g/L]
Na$_2$HPO$_4$.2H$_2$O	98.0%	0.505		0.363		[g/L]
MgCl$_2$.6H$_2$O	99.0%		0.616		0.616	[g/L]
HCl (1.0 M)	100.0%		1.92		2.40	[mL/L]
CaCl$_2$	97.0%		0.529		0.572	[g/L]
Na$_2$SO$_4$	99.0%	0.143		0.143		[g/L]

Table S2. Composition of SBF-BCS.

Solution	Na$^+$	K$^+$	Mg^{2+}	Ca^{2+}	CO$_3^{2-}$	PO$_4^{3-}$	SO$_4^{2-}$	Cl$^-$
BCS-1 [mM]	143.00	--	1.50	2.31	22.20	1.39	0.50	124.64
BCS-2 [mM]	142.0	5.0	1.5	2.5	22.6	1.0	0.5	130.6

Figure S1. Recommended setup for apatite forming ability test of samples of rectangular shape (a) and circular shape (b).
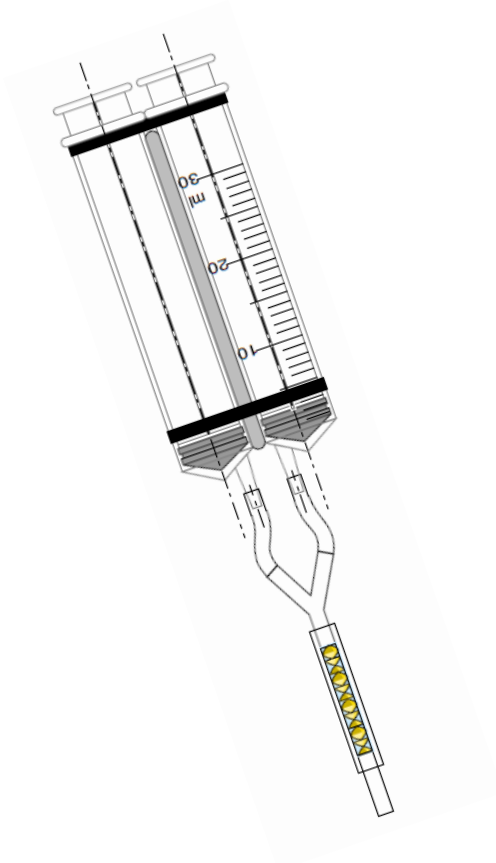
Figure S2. Twin syringes used for mixing solution A and B for apatite forming ability test.

### 3. Apatite forming ability of four Ti surfaces in different SBFs
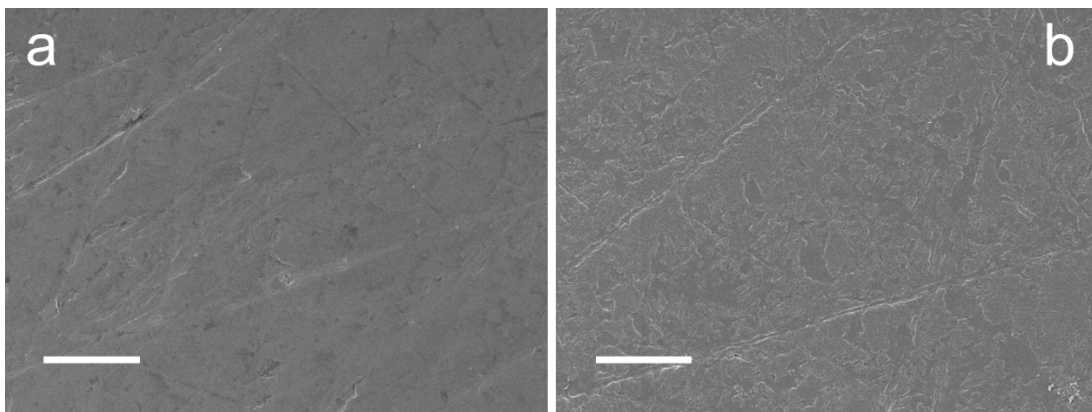
Figure S3. SEM images of as-polished Ti (a) and polished, heat treated Ti (b) tested in BCS-2 without BSA for one week. No HA was found on both samples. Similar morphologies were observed for each material tested in all other solutions. Scale bars are 10 µm.

4. Kinetic study of the effect of BSA at different concentrations
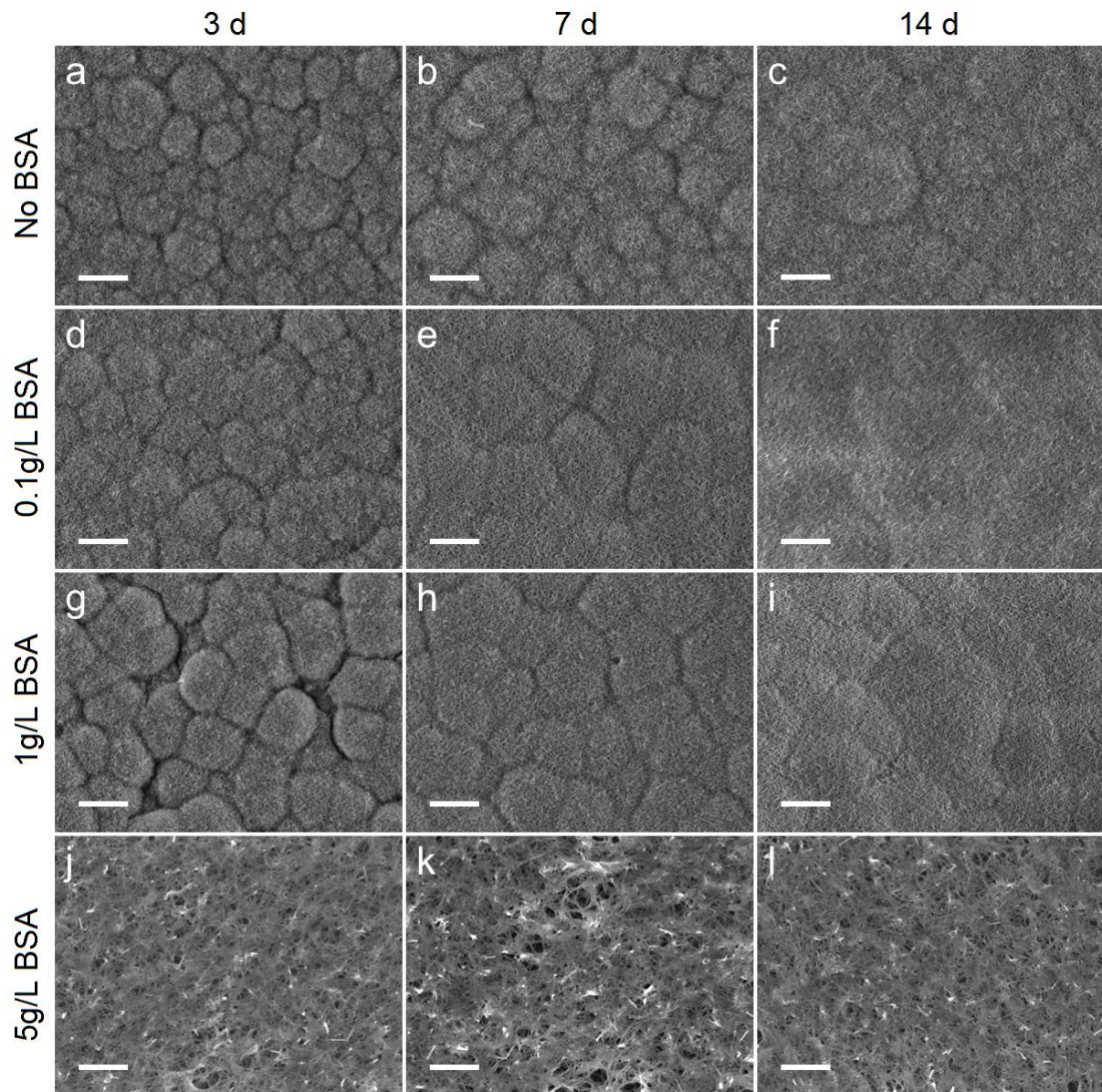
Figure S4. SEM images of NaOH treated Ti after immersion in BCS-2 with protein concentrations at 0g/L for 3d (a), 7d (b), 14d (c); 0.1g/L for 3d (d), 7d (e), 14d (f); 1g/L for 3d (g), 7d (h), 14d (i) and 5g/L for 3d (j), 7d (k), 14d (l). Apatite formation can be determined by the presence of globules consisting of tiny flake-like crystals. No apparent morphology differences were observed irrespective of the addition of BSA. At the concentration of 5g/L BSA, only the porous surface can be seen, showing a complete inhibition of HA formation. All scale bars are 2 μm.
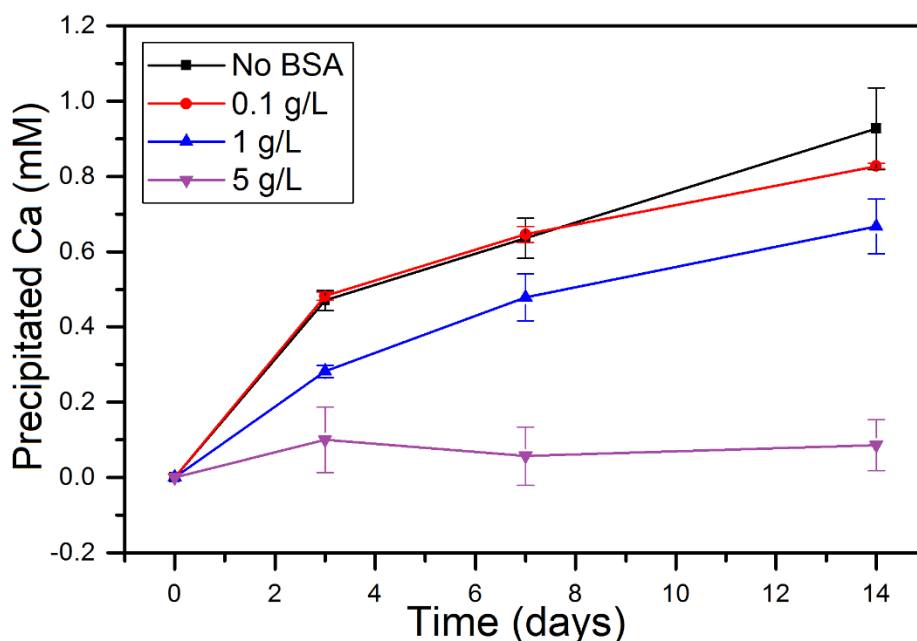
Figure S5. Plot of the HA growth on NaOH treated Ti in BCS-2 with different protein concentrations. The error bar is the standard deviation calculated based on two replicates.

5. Effect of BSA on solution free calcium concentration

Table S3. Measurement of free calcium concentrations with and without the presence of BSA.

| BSA (g/L)	Ca concentration (mg/L)	
	Measurement 1	Measurement 2
0	110.4	111.8
1	113.8	115.5
5	112.5	112.9
10	108.9	108.0
20	100.6	101.4

A good linear fit of free Ca^{2+} ion concentrations in solutions with BSA can be obtained, showing a decrease of free calcium ions with the presence of BSA. However, without BSA, measured free calcium concentration is slightly lower than that at 1g/L BSA. This is likely an artifact of the measurements due to different electrode response as the increase in free calcium concentration in the presence of 1g/L BSA is physically unlikely due to a 100.00% (calculated) distribution of total calcium as free Ca^{2+} in BSA-free solution, thus could hardly release more Ca^{2+} when BSA is introduced. The Figure 8 in the main text is plotted by adjusting the free calcium concentration at 0g/L BSA using the extrapolation of the linear fit obtained with data collected from solutions containing BSA.

6. Effect of BSA on solution pH
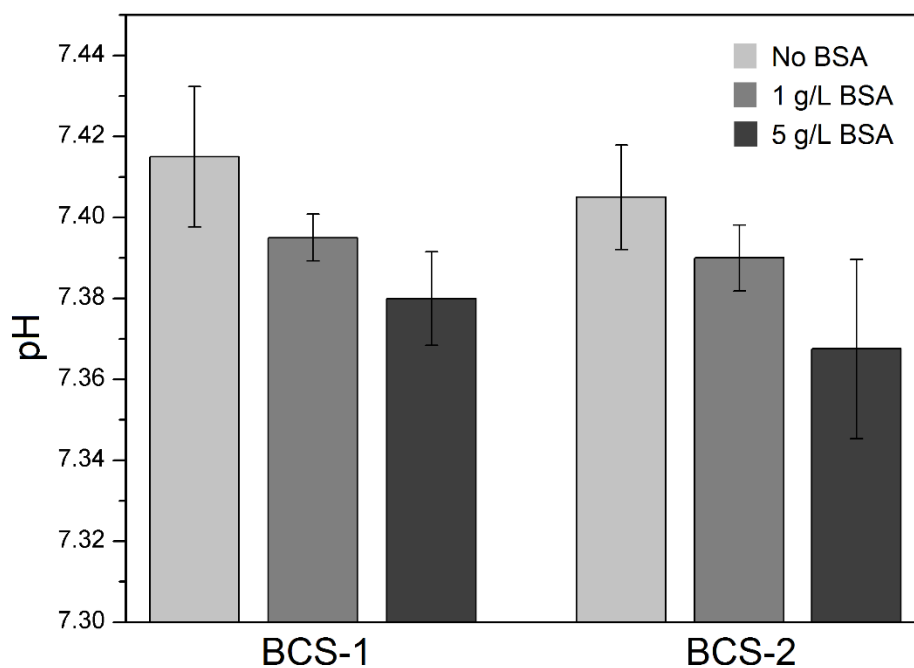
Figure S6. pH values measured of BCS-1 and BCS-2 without BSA and in the presence of BSA at 1g/L and 5g/L. The error bar is the standard deviation calculated based on four replicates.

7. Solution pH buffering capacity
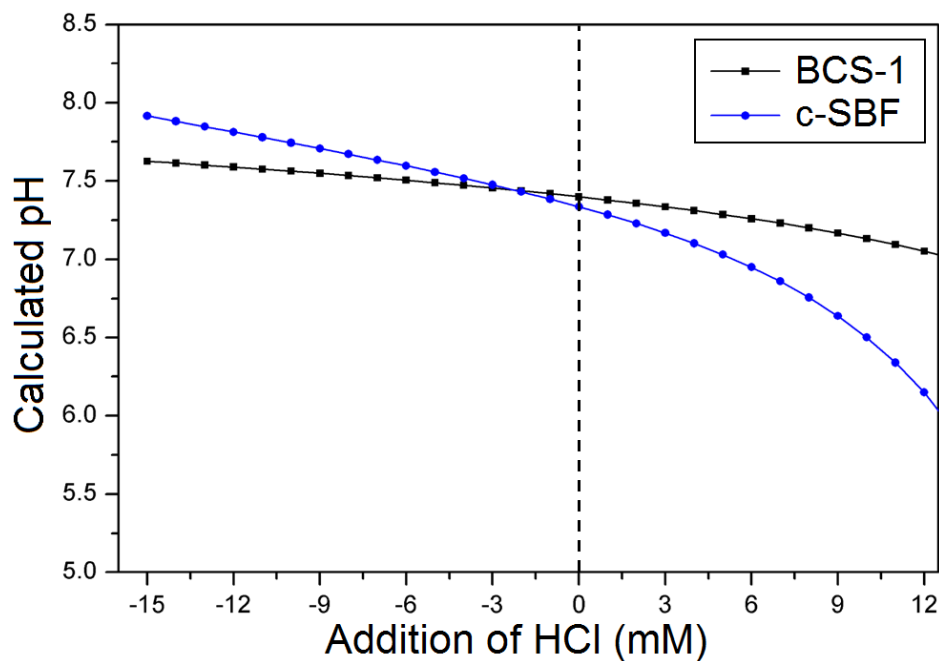
Figure S7. Calculated pH values of BCS-1 and c-SBF as a function of additional HCl. The negative values are calculated by replacing NaCl in the solution by NaOH. The dashed line is drawn at the exact SBF composition and indicates the solution pH without additional acid/base. The curve of BCS-2 overlaps with BCS-1 and is thus not included.

8. Stability test of BCS-1 and BCS-2

The solution BCS-1 and BCS-2 were prepared following the operating protocols and were placed into an incubator without the introduction of any samples. After 4 weeks, the solutions were quickly taken out and filtered through a 30 kDa ultrafiltration disc (Ultracel, Millipore) using a pressure cell (solvent-resistant stirred cell, Millipore) operating at 1.5 bar. Afterwards, the filtrate was then added with 1 vol% 65 wt% concentrated HNO_3 to prevent possible further calcium phosphate nucleation, and then taken for ICP-OES analysis for calcium and phosphorous. The use of the ultrafiltration membrane ensures that possible precipitates of calcium phosphate or calcium carbonate in the solution with sizes larger than a few nanometers can be trapped on the membrane, thus any homogeneous nucleation event (instability) would reduce the calcium concentration in the filtrate. This method however cannot filter ultra-small particles such as possible pre-nucleation clusters with sizes below 1 nm. Control solutions without incubation were also diluted with the same procedure and analyzed by ICP-OES. The results indicate that no significant instability of the solution were detected, as illustrated in Table S4 and Figure S8.

Table S4. Measured calcium and phosphorus concentration in filtrates.

|	Sample	Ca mg/L	P mg/L
BCS-1	Solution A	--	85.3
	Solution B	191.9	--
	Replicate 1	90.9	43.7
	Replicate 2	93.9	43.0
	Replicate 3	94.1	43.1
BCS-2	Solution A	--	70.0
	Solution B	190.0	--
	Replicate 1	90.7	35.7
	Replicate 2	92.5	37.1
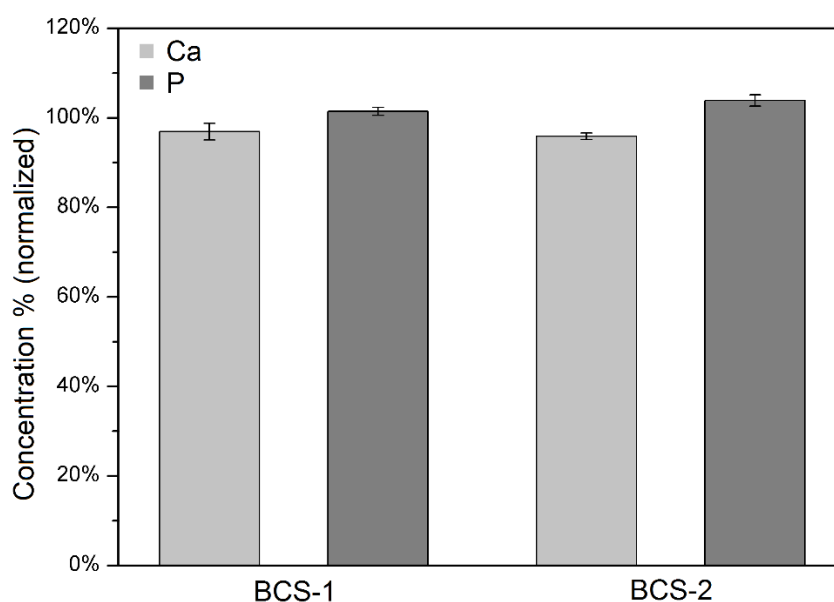
Figure S8. Plot of calcium and phosphorus concentrations after adjusting the dilution and normalizing to the values obtained from the control groups.

9. Effect of carbonates in c-SBF

For c-SBF, the degree of supersaturation with respect to HA is dependent on how much additional 1M HCl is added during the preparation and the extent of carbonate exchange with air, as the partial pressure of CO_2 in solution is higher than that of the air. The supersaturation can be calculated using the thermodynamic model and is shown in Figure S9. It should be noted that although in some regions the c-SBF has a higher supersaturation compared to BCS-1 and BCS-2, this does not necessarily mean that the solution is more active in precipitating HA. This is due to other factors such as the highly carbonated-HA formed in the cases of BCS-1 and BCS-2. The current calculation of supersaturation considers only stoichiometric HA.
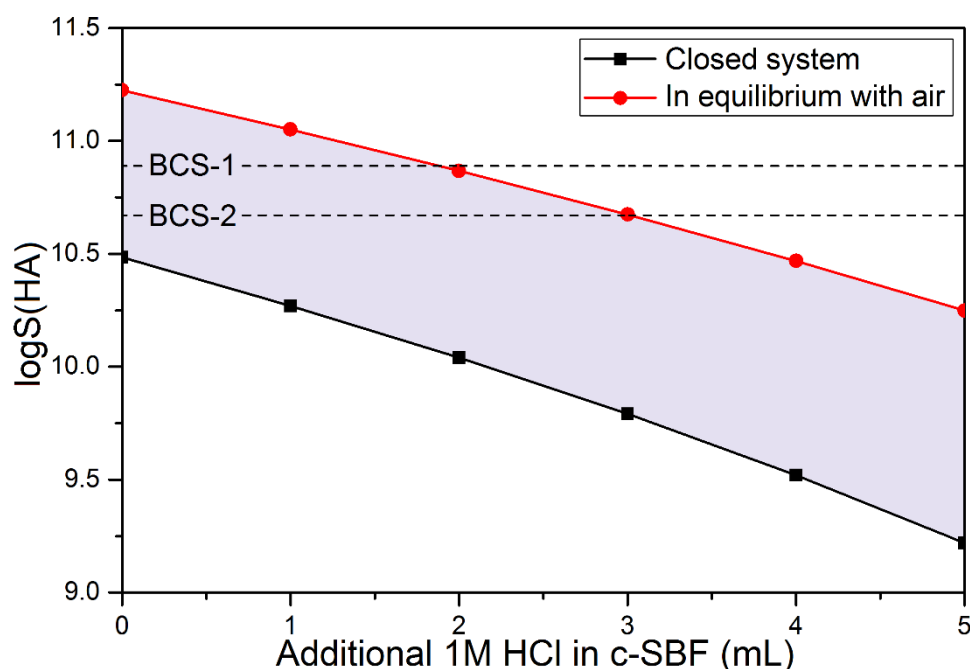
Figure S9. Plot of calculated supersaturation level with respect to HA in c-SBF as a function of additional 1M HCl added in preparation step 6 (ISO 23317), where 0 – 5 mL is recommended. The black dots are the calculated values assuming no exchange with atmosphere and red dots are calculated assuming complete equilibrium with air (solution CO_2 partial pressure reaches 0.04%). The purple region marks all possible values of logS(HA). The supersaturation level in BCS-1 and BCS-2 is marked by dashed lines for reference, and is not a function of additional HCl in c-SBF.

References

[1]   G. Vereecke, J. Lemaître, Calculation of the solubility diagrams in the system Ca(OH)$_2$-H$_3$PO$_4$-KOH-HNO$_3$-CO$_2$-H$_2$O, J. Cryst. Growth. 104 (1990) 820–832.

[2]   R.A. Robinson, R.H. Stokes, Electrolyte Solutions: Second Revised Edition, 2002.